Photomedicine and Laser Surgery
Volume 33, Number 3, 2015

Pp. 145–153
DOI: 10.1089/pho.2014.3744

Effect of Low-Level Laser Therapy in an Experimental Model of Osteoarthritis in Rats Evaluated Through Raman Spectroscopy

Nilton Maciel Mangueira, PhD,[1] Murilo Xavier, PhD,[2] Renato Aparecido de Souza, PhD,[3] Miguel Angel Castillo Salgado, PhD,[4] Landulfo Silveira, Jr., PhD,[5] and Antonio Balbin Villaverde, PhD[5]

Abstract

Objective: This work aimed to investigate the biochemical changes associated with low-level laser therapy (LLLT) using 660 and 780 nm, on a well-established experimental model of osteoarthritis (OA) in the knees of rats with induced collagenase, using histomorphometry and Raman spectroscopy. ***Materials and methods:*** Thirty-six Wistar rats were divided into four groups: control (GCON, $n=9$), collagenase without treatment (GCOL, $n=9$), collagenase with LLLT 660 nm treatment (G660, $n=8$), and collagenase with LLLT 780 nm treatment (G780, $n=10$). LLLT protocol was: 30 mW power output, 10 sec irradiation time, 0.04 cm^2 spot size, 0.3 J energy, 0.75 W/cm^2 irradiance, and 7.5 J/cm^2 fluence per session per day, during 14 days. Then, knees were withdrawn and submitted to histomorphometry and Raman spectroscopy analysis. Principal components analysis (PCA) and Mahalanobis distance were employed to characterize the spectral findings. ***Results:*** Histomorphometry revealed a significant increase in the amount of collagen III for the group irradiated with 660 nm. The Raman bands at 1247, 1273, and 1453 cm^{-1} (from principal component score PC2), attributed to collagen type II, and 1460 cm^{-1} (from PC3), attributed to collagen type III, suggested that the LLLT causes acceleration in cellular activity, especially on the cells that repair cartilage, accelerating the breakdown of cartilage destroyed by collagenase and stimulating the fibroblast to synthesize repairing collagen III. ***Conclusions:*** LLLT accelerated the initial breakdown of cartilage destroyed by collagenase and stimulated the fibroblast to synthesize the repairing collagen III, suggesting a beneficial effect of LLLT on OA.

Introduction

Osteoarthritis (OA) is a disease of synovial joints characterized by degenerative and reparative processes. Among the several joints affected, OA of the knee is the most common type of arthritis, and the major cause of chronic musculoskeletal pain and mobility disability in the elderly, which, therefore, presents a significant burden on healthcare provision.[1]

Currently, diagnosis of OA is performed based on the patient's overall clinical impression (pain stiffness, swelling, dysfunction, and presence of deformity) and radiographic data (joint space narrowing, osteophytes, subchondral cysts, and sclerosis).[2] However, a discrepancy was reported between the symptoms and radiographic findings.[3] The difficulties in diagnosis of OA are essentially caused by the complexity of this disease. Most cases of OA are identified only in the advanced stages. Therefore, for greater efficiency in the diagnosis and treatment of OA, new tools with greater objectivity of analysis need to be investigated and validated.

An efficient treatment of patients with OA of the knee requires a combination of pharmacological and nonpharmacological therapies.[4] Recently, low-level light therapy (LLLT) using either laser or light-emitting diodes arose as a therapeutic alternative. Several experimental clinical trials have demonstrated the effects of the laser photobiostimulation, showing reduction of pain and improving the microcirculation in patients with knee OA,[5] increased cell proliferation,[6] stimulation of collagen production by fibroblasts,[7] bone repair, and modulation of inflammatory markers.[8]

[1]Department of Physiotherapy, Universidade Federal do Piauí, PI, Brazil.
[2]Department of Physiotherapy, Universidade Federal do Vale do Jequitinhonha e Mucuri, MG, Brazil.
[3]Instituto Federal de Educação, Ciência e Tecnologia do Sul de Minas Gerais, Campus Muzambinho, MG, Brazil.
[4]Departamento de Biociências e Diagnóstico Bucal, Universidade Estadual Paulista Júlio de Mesquita Filho, SP, Brazil.
[5]Biomedical Engineering Institute, Universidade Camilo Castelo Branco, SP, Brazil.

Previous studies demonstrated that laser therapy exerts a positive influence on bone regeneration[9] and biosynthesis of arthritic cartilage.[10] Alves et al.[11] reported that laser therapy (780 nm) modulates inflammatory response both in the early and in the late progression stages of rheumatoid arthritis (RA). Da Rosa et al.[12] observed the formation of new blood vessels in the laser- treated groups (660 nm) on the 7th day of treatment.

Raman spectroscopy is an analytical technique suitable for the analysis of biological samples, allowing a precise information on biochemical and biomolecular changes associated with diseases in several bio-tissues.[13–16] Furthermore, Raman spectroscopy encounters less interference from water, eliminating the need for dehydrating the samples before analysis. This makes Raman spectroscopy especially advantageous for the characterization of changes in cartilage tissues, which are made up of 70% water.[17] Therefore, some studies have evaluated Raman spectroscopy as a technique for studying cartilage regeneration,[17–20] as well as diagnosing OA.[21,22] The potential of Raman spectroscopy in the diagnosis and detection of cartilage damage and monitoring of subchondral bone and bone in OA pathogenesis at the molecular level has been demonstrated.[23]

Traditionally, the composition of bone and cartilage is determined by standard histological methods. However, although much of the actual research work uses histological methods to show the effects of LLLT cartilage and subchondral bone destroyed by OA,[11,12] few studies employed Raman spectroscopy for this purpose. Abnormal molecular changes observed in the matrix of OA subchondral bone and proper cartilaginous matrix formation have been studied by means of Raman spectroscopy.[24] The cartilage and soft tissues constituents, as well as the quality of the remodeling in joint-related tissues, are being studied using some Raman markers as the bands in the intervals: 850–856 cm^{-1} (proline), 875–881 cm^{-1} (hydroxyproline), 1001–1003 (phenylalanine), and 1230–1280 cm^{-1} (amide III), corresponding to the organic matrix (collagen); 1060–1063 cm^{-1}, representing chondroitin sulfate, 957–962 cm^{-1} (hydroxyapatite), and 1065–1071 cm^{-1} (carbonated hydroxyapatite), representing mineral content.[17,21] Also, the use of ratios between the intensities or areas of selected Raman bands in order to describe the biochemical alterations in cartilaginous tissues is well documented.[16,17,21,25,26] Multivariate statistics such as principal components analysis (PCA), a technique suitable for data reduction and features extraction, when associated with Raman spectroscopy, can be used to reveal the biochemical constitution of biological tissues and for label-free detection of individual cartilaginous zones.[27] In addition, PCA has been used to characterize biological tissues with the aims of identification of biochemical composition and diagnosis.[28,29]

The aim of this study was to investigate the biochemical and biomolecular changes associated with LLLT on a well-established experimental model of OA (collagenase of the knee) in rats, in an attempt to elucidate the effects of LLLT on damaged cartilage using the spectral information provided by Raman spectroscopy, as this protocol had not been used before. With the characterization of the Raman features on the damaged cartilage after laser treatment by PCA, the framework for the analysis of cartilaginous tissue could be improved.

Material and Methods

Animals and experimental design

All experiments were conducted in accordance with internationally accredited guidelines and were approved by the Research Ethics Committee for animal care of the Universidade Federal do Vale do Jequitinhonha e Mucuri (UFVJM) (protocol no. 011-2010). The experiment employed 36 males Wistar rats (220–260 g), provided by the bioterium of the Department of Animal Research of the UFVJM. All animals were individually placed in appropriate cages and kept in the bioterium temperature (22 ± 3°C), relative humidity (60 ± 10%), 12 h/12 h light/dark cycle, and supplied with food and water *ad libitum* during the experimental period of 18 days. Animals were randomly divided into four experimental groups as follows: control group (GCON, $n = 9$), the animals received intra-articular injection of saline solution; collagenase group (GCOL, $n = 9$), the animals received intra-articular injection of collagenase; laser 660 nm group (G660, $n = 8$), the animals received collagenase and were treated with LLLT 660 nm; and finally, laser 780 nm group (G780, $n = 10$), the animals received collagenase and were treated with LLLT 780 nm.

Collagenase-induced model of OA

For the induction of collagenase in the OA model, the animals were previously anesthetized by intraperitoneal application of xylazine HCl 2% (Xilazin 2%, Syntec do Brasil, São Paulo, Brazil) and ketamine HCl 10% (Cetamin 10%, Syntec do Brasil, São Paulo, Brazil), both at a concentration of 0.1 mL per 100 g body weight. OA was induced by intra-articular injection of collagenase (*Clostridium histolyticum* type II, enzyme activity of 333 U/mg, Sigma Co., St. Louis, MO). Collagenase was dissolved in sterile saline phosphate buffer (50 mM of NaH_2PO_4 and 150 mM of NaCl, pH 7.4). After shaving and sterilizing, the right knee joint of the GCOL, G660, and G780 groups was injected intra-articularly with 0.1 mL of collagenase (500 U) using a 27 gauge, 12.7 mm long needle. Injections for each animal were performed on the 1st and the 4th days of the experiment, respectively, according to the protocol of Lee et al.[30] The GCON group received 0.1 mL of saline solution without collagenase.

Laser therapy

LLLT started 12 h after the second injection of collagenase (4th day), according to the previous study, which started treatment on collagenase-induced tendinitis after 12 h,[31] and was repeated daily, during 14 days. The equipment used in the study was a Twin Flex Evolution (MMOptics, São Carlos, SP, Brazil), possessing laser wavelengths of 660 and 780 nm. For the irradiation procedure, animals were positioned on a table and manually immobilized. For each group being laser irradiated, the laser was applied directly on the injury, perpendicularly to the tissue surface and punctual, with the following laser parameters: 30 mW power output, 10 sec irradiation time, 0.04 cm^2 spot size, 0.3 J energy, 0.75 W/cm^2 irradiance, and 7.5 J/cm^2 fluence. The animals in groups GCON and GCOL were subjected to the same procedure, with the laser turned off.

Specimen preparation

On the 19th day, all rats were anesthetized with an intramuscular administration of 40 mg/kg xylazine HCl and

50 mg/kg ketamine HCl and euthanized with an intracardiac injection of KCl solution (KCl 10%; Laboratório Ariston, São Paulo, Brazil). The right tibial plateau of each rat was dissected with removal of the soft tissue, joint capsule, and central knee ligaments, exposing the articular cartilage (tibial), leaving no residue on the surface. In the sequence, samples were stored at −80°C (in a freezer) until spectral analysis. In order to evaluate alterations in the articular surface area, the menisci-covered tibial region (medial tibial plateau) was assessed. Prior to Raman experiments, the samples were gradually warmed up to room temperature with a saline solution, and their surfaces adequately positioned in the Raman spectrometer without any chemical fixation or treatment.

Raman spectroscopy analysis

Raman spectra were obtained at the medial tibial plateau of all experimental groups using a dispersive micro-Raman spectrometer (model Dimension P1, Lambda Solutions, Inc., MA) (Fig. 1). The Raman system operated with an 830 nm, 350 mW (adjustable) diode laser for sample excitation, a 1200 lines/mm grating, and a deep-depleted 1340 × 100 pixels charge-coupled device (CCD) camera (−75°C, Peltier cooling) for signal collection, resulting in a spectral resolution of $\sim 2\,cm^{-1}$ in the spectral range of 400–1800 cm^{-1}, where the most relevant features of bone are seen.[32] A notebook computer hosts the software (RamanSoft®, version 1.7, Lambda Solutions, Inc., MA) used for data acquisition, storage, and spectral analysis. This Raman system employs an optical microscope, with suitable excitation and collection filters, which guarantees repeatability in emission/collection geometry with laser power stability, by means of a 10× microscope objective. For Raman measurements, integration time was adjusted to 20 sec for all samples. The laser power from the Raman system measured at the sample surface was ~200 mW, not sufficient to provoke tissue damage (burning), as cartilaginous tissue presents lower absorption with 830 nm, ranging from 0.1 to 0.01 cm^{-1}, with pulse duration long enough for thermal diffusion.[33] Both intensity and wave number were calibrated before each experiment, using the Raman bands of naphthalene.

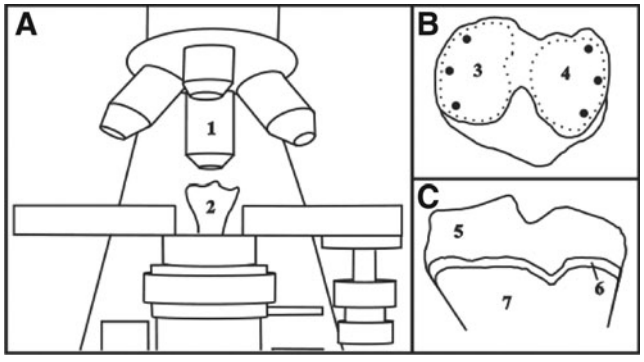

FIG. 1. Micro-Raman measurements on the surface of the right knee of rats. **(A)** Micro-Raman with the right tibia in place and the data collection by means of a 20× objective (1) and position of the right tibia from the anterior view (2). **(B)** Spots of the Raman collection at the surface of the medial (3) and lateral (4) tibial plateau from the top view. **(C)** Coronal cut of the tibial plateau articular cartilage showing the right layer (5), transition zone (6), and subchondral bone (7).

As shown in Fig. 1, the Raman spectrum was obtained at the surface of the medial (3) and lateral (4) tibial plateau, in three points of each side of the articular cartilage, totaling 6 spectra for each cartilage and 216 spectra for the whole data set (6 spectra in 36 animals). Spectra were submitted to preprocessing procedures. First, background fluorescence emission was removed by fitting and subtracting a fifth order polynomial to the spectrum in the studied spectral range using OriginPro® (Origin Lab Corp., MA, version 7.5). Then, the cosmic ray spikes were manually removed using Microsoft Excel 2003® (Microsoft Corporation, Arvato Distribution GmbH, Herzebrock-Clarholz, DE).

The mean Raman spectra of all groups were then plotted, and the spectral parameters that could be related to cartilage, subchondral bone, and bone molecular changes were induced by LLLT, were extracted from the data set using PCA.

The spectral parameters resulting from PCA, the principal components scores (SCs) and the loading vectors (PCs), were used to correlate the changes in tissue biochemistry caused by the OA induction and LLLT effects. These loading vectors resemble Raman spectra and the first ones present the differences in the features that could discriminate each group.[34] Scores are the intensities of each PC in each spectrum, so any difference in the PCs of each group can be observed through the differences in the SC associated to that PC.

The spectral features of each PC were confronted with the known biochemical composition of the cartilage. The possible differences between the means of the SCs of each experimental group were evaluated by one-way analysis of variance (ANOVA) with significance level of 5%, with post-hoc analysis (Tukey–Kramer test for parametric or Dunn test for nonparametric data), preceded by a normality test, used to determine which group had the difference in the SC. ANOVA was performed using Instat 3.0® (Graphpad Software Inc., CA) whereas PCA was calculated through the princomp.m routine in Matlab 6.2, Statistics Toolbox® (Mathworks, MA).

Histomorphometric analysis

After Raman analysis, the tibias were placed in buffered formaldehyde 4%, pH 7.4, at 4°C for 24 h. The tissues were then decalcified in a solution of ethylenediamine tetra-acetic acid (EDTA) at 40% for ~30 days, and included in paraffin blocks. Each block was sawed by half in the frontal plane perpendicular to the cartilage surface and cut into 6 μm, not successive, slices. Thirty- six histological blades were prepared and stained with picrosirius red (PR) for measuring the area of cartilage collagen.[35] For each blade, four images were captured under polarized light microscopy (model DM LB2®, Leica do Brasil, São Paulo, Brazil) with a 20× objective, totaling 144 images. All images were analyzed using ImageJ (National Institutes of Health®, Bethesda, MD, version 1.48). Areas with collagen fibers were determined in the image using the color segmentation in ImageJ, where the collagen fibers are visible by their color because of birefringence.[36] The fibers of collagen type II were identified as yellowish (RGB color: R: 220, G: 205, B: 103), whereas the collagen type III fibers were identified as greenish (RGB color: R: 114,

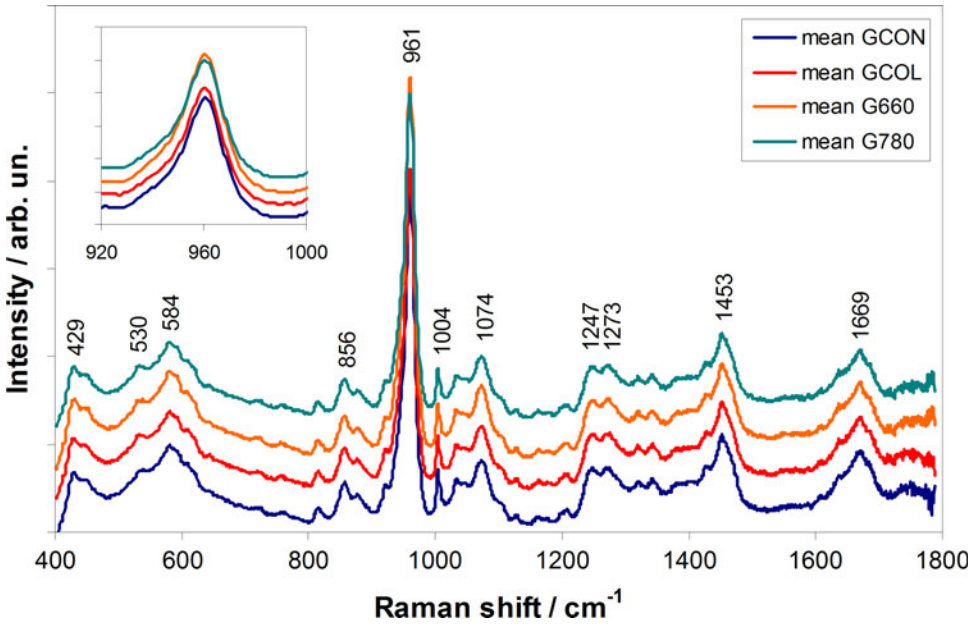

FIG. 2. Mean Raman spectra of the control group (GCON), the collagenase without treatment group (GCOL), the collagenase with LLLT 660 nm treatment group (G660), and collagenase with LLLT 780 nm treatment (G780), with main peaks related to the constitution of cartilage and subchondral bone from joint. Inner plot evidences differences in the intensity of the 961 cm^{-1} peak of hydroxyapatite. Spectra were offset for clarity.

G: 114, B: 82). The same color settings were used for all analyzed groups.

Results

Raman spectroscopy

Figure 2 presents the mean Raman spectra of the tibial plateau for the groups GCON, GCOL, G660, and G780. The Raman spectra of cartilage joint is dominated by bands of hydroxyapatite from subchondral bone at 960 and 1072 cm^{-1} (phosphated and carbonated hydroxyapatite, respectively) and bands of organic matrix (collagen) at 856, 1004, 1247, 1273, 1453, and 1669 cm^{-1} (proline/hydroxyproline, phenylalanine, amide III, amide II, CH_2 modes, and amide I, respectively). No differences in the peak positions among the groups were observed, although differences in the intensity of the hydroxyapatite peaks were seen, being that G660 presented increased intensity and GCOL decreased intensity both compared with GCON. Table 1 summarizes the band assignment of the major Raman peaks of cartilage and bone spectra.[18,20,32,37]

To estimate the changes associated with LLLT in collagenase-induced OA, multivariate statistics PCA was employed. Figure 3 shows the Raman spectra of PCA loading vectors (left) and PCA scores (right). The spectral features presented in the first PC vectors show Raman bands of main constituents of joint bone/cartilage (collagen) and differences in the PC scores indicate chemical changes induced by the action of LLLT. PC1 vector shows (Fig. 3a) the spectral characteristics of bone (protein matrix and apatite features) and cartilage (protein features including collagen and chondroitin sulfate). PC2 vector (Fig. 3c) presents spectral features of proteins, with positive peaks, and the band of phosphated apatite, with a negative peak. PC3 vector (Fig. 3e) also presents remnant bands of proteins and an interesting negative band at 966 cm^{-1} (band of hydroxyapatite). PC4 and PC5 (Fig. 3g and 3i, respectively) have bands related to hydroxyapatite. The spectral differences in the groups are highlighted mainly by PC1, PC2, and PC3. The protein bands in PC2 are compatible with collagen type II, and the ones in PC3 are compatible with collagen type III.

In terms of the intensity of each principal component, the PC1 score (Fig. 3b) highlighted the presence of the peak of phosphate from the bone mineral in the sample and general features of proteins (collagen), with higher intensity for the G660 ($p < 0.05$). The PC2 score (Fig. 3d) indicated a decreased amount of organic material with spectral feature suggestive of collagen II in the groups treated with LLLT. The PC3 score

TABLE 1. BAND ASSIGNMENTS FOR THE COMPONENTS FROM CARTILAGE (C), SUBCHONDRAL BONE (SB), AND CANCELLOUS BONE TISSUE (B)[17,19,33,31]

Raman shift (cm^{-1})	*Spectral assignment*	*Component*	*Tissue*
856	C-C stretch – proline/hydroxyproline ring	Collagen matrix	C, SB
961	PO_4^{3-} stretch – phosphated hydroxyapatite	Apatite mineral	B
1004	C-C symmetric ring stretch – phenylalanine	Collagen – matrix	C, SB
1074	CO_3^{2-} stretch – carbonated hydroxyapatite	Apatite mineral	B
	SO^{3-} symmetric ring stretch (at 1063 cm^{-1})	Chondroitin sulfate	C
1247, 1273	C-N and N-H modes of amide III envelope (1230 - 1300 cm^{-1})	Collagen – matrix	C, SB
1453, 1460	CH_2/CH_3 deformation	Proteins (collagen), lipid	C, B
1669	C=O stretch of amide I	Collagen	C, SB

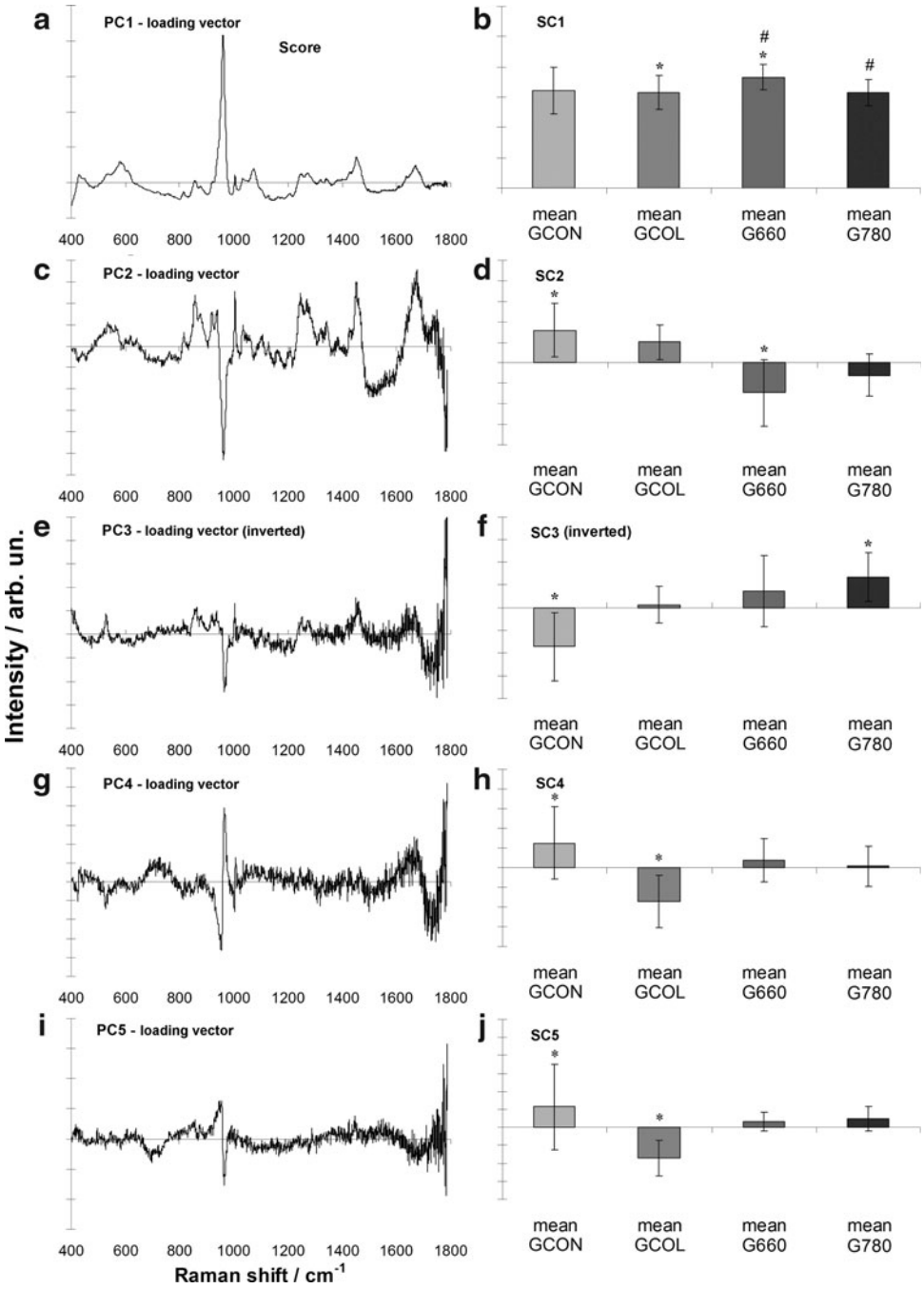

FIG. 3. Plot of the loading vectors (*left*) and scores (*right*) of the first five principal components for the Raman spectra used in the principal components analysis (PCA). The spectral features observed in the loading vectors relate to the features of joint bone/cartilage tissue. * and # indicate groups with statistically significant differences ($p < 0.05$) between means evaluated by analysis of variance (ANOVA)/ Tukey–Kramer test.

(Fig. 3f) indicates an increase of proteins with spectral features that resemble the collagen III. Finally, the PC4 and PC5 scores (Fig. 3g and j, respectively) show differences in the inorganic content, related to the subchondral bone.

In order to discriminate the groups based on the differences of the PC scores, scatter plot of PC2 score versus PC3 score was shown in Fig. 4. PC2 and PC3 scores were chosen because they showed a higher discrimination capability by ANOVA ($p < 0.05$). It can be seen that the GCON and GCOL groups can be separated from each other with high discrimination by means of Mahalanobis distance, and the treatment groups (G660 and G780) can be separated from the GCON and GCOL groups also with high discrimination. This discrimination capability is justified by the fact that the score of each principal component can be related to the concentration of the biochemical component presented in the tissue, and this discrimination attests that there are biochemical differences among the experimental groups.

Histomorphometric analysis

Figure 5a shows the areas of collagen II and collagen III obtained for each experimental group. For the GCOL group, a significantly lower amount of both collagen II and III compared with GCON ($p < 0.05$) was found. Furthermore, the collagen III area of G660 was significantly higher than that for GCOL and G780 ($p < 0.05$, for both). A higher amount of collagen III compared with collagen II was found

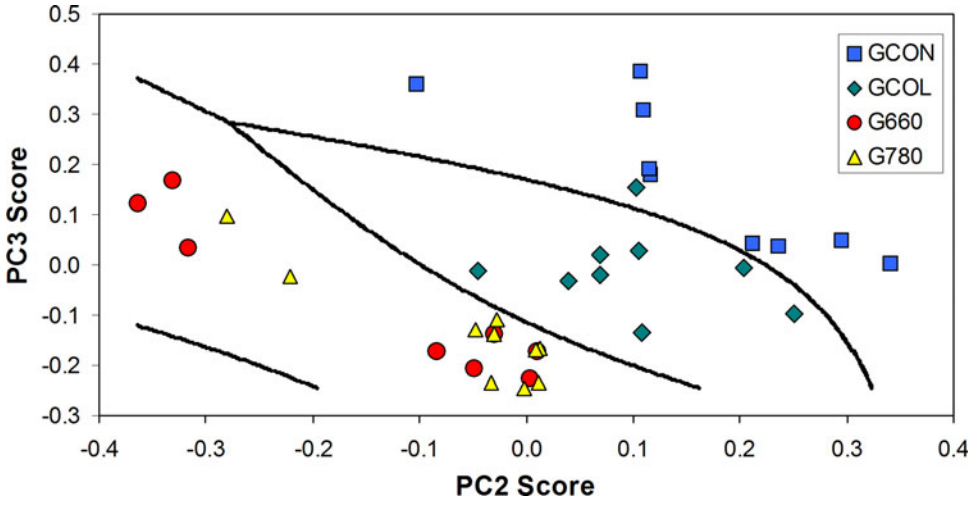

FIG. 4. Binary plot of the PC2 score versus the PC3 score, showing the discrimination among the control group (GCON), the collagenase without treatmen group (GCOL), the collagenase with LLLT 660 nm treatment group (G660), and collagenase with LLLT 780 nm treatment group (G780), using the Mahalanobis distance as a discriminator.[27]

in group G660 ($p<0.05$). Although not statistically significant, the amount of collagen II was increased for both G660 and G780 compared with GCOL, and the amount of collagen III was higher for G780 than for GCOL. These results denote that laser 660 nm (G660) stimulated cell proliferation and synthesis of collagen III, repairing cartilage damaged by the collagenase than the 780 nm laser (G780). Figure 5b displays the correlation between the intensities of the principal components that present the significant features of protein and hydroxyapatite (PC2 + PC3) with the total cartilage area of collagen (collagen II + collagen III). Correlation coefficient $r=0.85$ indicates that Raman features extracted by PCA could be correlated to the amount of collagen synthesized by laser-induced cell proliferation.

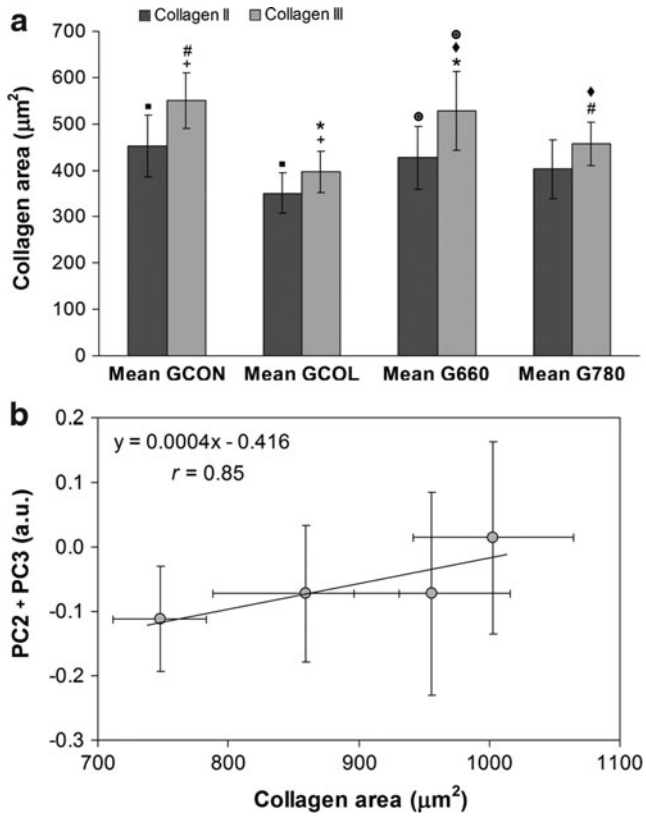

FIG. 5. **(a)** Histomorphometric analysis of articular cartilage of rat knee, presenting significant difference between the mean areas of collagen types II and III for the four experimental groups. **(b)** Plot of the correlation between the intensities of the principal components (PC2 + PC3) with the total area of collagen (collagen II + III) of the histomorphometric study. Symbols indicate statistically significant differences ($p<0.05$) between corresponding groups.

Discussion

To our understanding, this is the first time that the effects of LLLT on collagen-induced OA were investigated using Raman spectroscopy. The Raman technique was selected because all treatment depended upon the ability to identify OA at a stage when it was potentially reversible, and to detect small changes in cartilage structure and function that had not been possible using conventional imaging techniques.[34,38] Therefore, the purpose of this study was to examine the effects of LLLT on Raman bands of damaged cartilage tissue through PCA analysis.

The key findings of the current study indicated that Raman spectroscopy associated with multivariate statistical analysis PCA identified that LLLT affected OA collagenase-induced pathogenesis. Recently, our research group showed the feasibility of applying Raman spectroscopy in probing the molecular changes in terms of collagen deposition and tissue remodeling associated with two well-established experimental models of OA in the knees of rats.[23] Intensities of the Raman bands of collagen, chondroitin sulfate, and mineral content, as well as analyses of ratios related to the quality of cartilage, were considered important for understanding how the experimental models of OA could act in joint tissues.[23]

It was suggested in the literature that Raman spectroscopy might be useful for recognizing and quantitatively assessing the degree of OA in its early stage. Five arthritic human tibial cartilages retrieved after total knee arthroplasty were examined. Raman spectra were then collected from selected zones with different damage severities. An increase in the relative intensity ratio between the Raman bands at 1241 and 1269 cm^{-1} (amide III) was observed with increasing

degradation grades, which could be related to structural changes in collagen type II under loading.[39]

Feasibility of Raman spectroscopy to effectively detect a wide spectrum of biomolecular changes associated with cartilage damage, prior to visible histological changes, has been shown.[17] It is important to note that articular cartilage is composed of chondrocytes and extracellular matrix consisting of 70–80% water, collagen type II (composed mainly of proline, hydroxyproline and phenylalanine), glycosaminoglycans (GAG), and proteoglycans (mainly consisted of aggrecan).[40] Structural analysis of GAG and proteoglycans by Raman microspectroscopy revealed that spectrum of aggrecan is dominated by chondroitin sulfate contribution ($1063\,cm^{-1}$).[18] Therefore, this Raman band could be used as a specific marker of cartilage.[17,20] However, it has been shown that chondroitin sulfate and collagen fibers had no significant molecular change in OA specimens compared with normal tissues.[23] Because we did not find significant differences between the band intensities and ratio of the mineral and organic (matrix) phase used as Raman markers (results not shown), we employed multivariate technique PCA to better characterize the spectral findings.

Unlike the analysis of the intensity of selected bands, multivariate analysis such as PCA has the ability to extract spectral features related to changes in the sample and to correlate with the disease. PCA is a statistical method used to reduce the dimensionality of the data set; that is, when a great number of variables (Raman wavenumbers) are obtained and a small number of variables (Raman features) are intended to explain the changes in the group caused by a disease, for example, and this reduced number of variables may present correlated information within the sample group.[27–30,41] PCA separates the data set into two new, uncorrelated variables (prinicpal components scores and loading vectors), based on their variance. PCA has been used as a tool to discriminate differences in the spectra of several biological materials, such as skin cells, bacteria, and body fluids.[29,42] In addition to the reduction in the number of variables, decomposition through PCA has also the ability to detect differences in the spectra caused by changes in the chemical constitution, using a suitable discrimination technique.[29]

Results of the present study have pointed out that PC1 vector reveals especially the mineral content from subchondral bone and general features of protein from bone and cartilage, whereas PC2 and PC3 vectors indicate the organic content, mainly collagens II and III, respectively. The results indicate that LLLT increases collagenase activity, as is suggested by the decrease of the PC2 score for groups subjected to LLLT, and favoring the exposure of the subchondral bone area, caused by the increased intensity of the PC1 score. Likewise, the higher intensity of the PC3 score reveals the beginning of the cartilage repair process.

It has been reported by Sobol et al.[43] that LLLT causes acceleration in cellular activity, especially on the cells that repair cartilage, accelerating the breakdown of cartilage destroyed by collagenase. Therefore, with the destroyed cartilage layer, the subchondral bone stays highlighted, which shows a prominent peak of phosphate,[23] as observed in the PC1 score. On the other hand, the lower values obtained for the PC2 score indicate a small organic content of the groups treated with LLLT. Considering that LLLT was started immediately after inflammation induction and that it continued during the higher cellular activity period, it is reasonable to assume that 14 days of LLLT caused a ''clean out'' of the collagenase-induced debris. Evidence of the increase in anabolic and catabolic activity occurs in the initial days following injury and lasts 2 weeks, at which point these levels diminish.[44]

LLLT seems to have increased cell activity, accelerating the cartilage destruction by the action of collagenase, and exposing the subchondral bone area, as is evidenced by the higher intensity of the PC1 score for the G660 group and the lower intensity of the PC2 score for the LLLT groups, markedly the G660. Likewise, the spectral information presented in the PC3 score, with the presence of spectral features of collagen III, is suggestive of being part of the beginning of the cartilage repair process injured by collagenase, because the PC3 scores are increased for the LLLT groups. The negative band at $\sim 961\,cm^{-1}$ in PC4 and PC5 (Fig. 3g and i, respectively) may indicate an increased exposure of the subchondral bone because of the destruction of the organic matrix by collagenase.

Raman outcomes indicate that there is a wavelength dependence, evidenced by the fact that results for the G660 group were different than for the G780 group. Wavelength dependence was also observed by Da Rosa et al.,[12] which obtained higher intensity of inflammatory cells in the group treated with laser 660 nm when compared with the 808 nm group in an experimental model of papain-induced OA. Also, they observed that 808 nm radiation stimulated angiogenesis and reduced the formation of fibrosis. That information, associated with the findings of the present study, suggest a better beneficial effect on OA for the 660 nm laser as compared with the 780 nm laser.

Hyaline articular cartilage is basically cells (chondrocytes) and ECM, forming the framework of the organic macromolecular matrix.[43] In our study, histomorphometry showed that the laser, especially 660 nm (G660), stimulated an increase of collagen III fibers. These collagen fibers were more prevalent in all irradiated groups, contributing to the repair of damaged cartilage. Histomorphometric results showed a positive correlation of the area of collagen fibers compared with the Raman spectra found through the PC scores; that is, the Raman features identified an increased amount of collagen II and III in irradiated tissues. These data are consistent with the literature, which shows that articular cartilage has networks of disorganized collagen and lower quantities in the advanced stage of OA.[45,46] In OA pathophysiology, the presence of type III collagen accelerates the degradation of type II collagen.[47] Several studies, clinical and experimental, have shown the effects of laser photobiostimulation in increased cell proliferation and repair cartilage tissue.[48,49]

Scanty cellular sources and low metabolic rate, along with a vascularity of cartilage, contributed to cartilage decreased regeneration ability. According to Sobol et al.[43] the efficacy of any approach aimed at controlling the regeneration process depends upon three tasks: (1) the ability to reproduce the normal cell differentiation sequence from the progenitor cells to mature chondrocytes; (2) stimulation of the specific subpopulations of the resident cells to proliferation and/or new matrix production, and (3) achievement of adequate spatial organization of the new growing tissue. It is probable that the most important feature of LLLT is the involvement and activation of the intrinsic mechanism of

cartilage repair. Although many studies were undertaken to verify the use of LLLT on cartilage functional state and reparative ability in OA, those studies have produced divergent results, mainly because of the wide range of wavelengths employed, power and energy densities of laser radiation, and different localizations of the irradiated area.[12]

Raman spectroscopy has been presented as a promising technique for the analysis of OA. It is possible to identify the molecular structure from the extraction of the corresponding vibration information. The acquisition of Raman spectra is fast and its result is molecular specific. As the size of the spot on the sample irradiated by the Raman excitation source is small and well defined by the micro-Raman focus, it is possible to carry out precise measures of tissue remodeling from the center to the edge of the sample. However, the application of Raman, especially micro-Raman, should be quite careful, because the final results of the analysis may be changed by impurities and fluorescences, and when the safety threshold is not obeyed, intense laser irradiance/fluence may lead to destruction of the sample by heating.

The present study, in addition to demonstrating that Raman spectroscopy could be a feasible method for assessment of damaged joint tissue composition, also showed that LLLT could act in collagenase-induced OA, particularly with employment of PCA and Mahalanobis distance analyses. It is likely that in the future, this Raman technique may be exploited to aid in the diagnosis of OA following magnetic resonance, facilitating the identification of the biochemical changes caused by the disease in clinics during knee surgery (arthroscopy), contributing to the speed and precision of the diagnosis and staging necessary for correct treatment, as well as monitoring the effects of different therapies, such as LLLT.

Conclusions

Raman spectroscopy was effective in identifying the molecular damage caused by the action of collagenase on the surface of articular cartilage in the knees of rats, causing OA. The scores of the PCA multivariate statistics pointed out that the PC1 loading vector was associated with the mineral content from subchondral bone, whereas PC2 and PC3 vectors pointed out the organic content of samples, mainly collagen types II and III. PCA scores suggested that LLLT stimulated cellular activity of cartilage repair and collagen synthesis, accelerating the breakdown of cartilage destroyed by collagenase and stimulating the fibroblast to synthesize repairing collagen III (higher intensity of PC3 score). Histomorphometric analysis showed that laser irradiation stimulated an increase of collagen III fibers in all irradiated groups, being more prevalent for the group treated with the 660 nm laser. Raman spectroscopy showed positive correlation with results obtained by histomorphometric analysis, related to the number of total cells (chondrocytes) as well as the increase in collagen area. These findings suggest that there is a beneficial effect of LLLT (mainly at 660 nm) on cartilage repair in OA.

Acknowledgments

R.A. Souza thanks Fundação de Amparo a Pesquisa do Estado de Minas Gerais (FAPEMIG) for research grant support (grant no. APQ-02900-10). M. Xavier thanks FAPEMIG for research grant support (grant no. APQ-01733-11). L. Silveira Jr. thanks São Paulo Research Foundation (FAPESP) for partial financial support (grant no. 2009/01788-5).

Author Disclosure Statement

No competing financial interests exist.

References

1. Neogi T. Clinical significance of bone changes in osteoarthritis. Ther Adv Musculoskelet Dis 2012;4:259–267.
2. Mobasheri A. Osteoarthritis year 2012 in review: biomarkers. Osteoarthr Cartilage 2012;20:1451–1464.
3. Bedson J, Croft PR. The discordance between clinical and radiographic knee osteoarthritis: A systematic search and summary of the literature. BMC Musculoskelet Disord 2008;2:9–116.
4. Zhang W, Moskowitz RW, Nuki G, et al. OARSI recommendations for the management of hip and knee osteoarthritis, Part II: OARSI evidence-based, expert consensus guidelines. Osteoarthr Cartilage 2008;16:137–162.
5. Hegedus B, Viharos L, Gervain M, Gálfi M. The effect of low-level laser in knee osteoarthritis: a double-blind, randomized, placebo-controlled trial. Photomed Laser Surg 2009;27:577–584.
6. Pallotta RC, Bjordal JM, Frigo L, et al. Infrared (810-nm) low-level laser therapy on rat experimental knee inflammation. Lasers Med Sci 2012;27:71–78.
7. Samoilova KA, Zhevago NA, Petrishchev NN, Zimin AA. Role of nitric oxide in the visible light-induced rapid increase of human skin microcirculation at the local and systemic levels: II. healthy volunteers. Photomed Laser Surg 2008;26:443–449.
8. Ré Poppi R, Da Silva AL, Nacer RS, et al. Evaluation of the osteogenic effect of low-level laser therapy (808 nm and 660 nm) on bone defects induced in the femurs of female rats submitted to ovariectomy. Lasers Med Sci 2011;26:515–522.
9. Barbosa D, de Souza RA, Xavier M, da Silva FF, Arisawa EA, Villaverde AG. Effects of low-level laser therapy (LLLT) on bone repair in rats: optical densitometry analysis. Lasers Med Sci 2013;28:651–656.
10. Lin YS, Huang MH, Chai CY. Effects of helium-neon laser on the mucopolysaccharide induction in experimental osteoarthritic cartilage. Osteoarthr Cartilage 2006;14:377–383.
11. Alves AC, de Carvalho PD, Parente M, et al. Low-level laser therapy in different stages of rheumatoid arthritis: a histological study. Lasers Med Sci 2013;28:529–536.
12. Da Rosa AS, dos Santos AF, da Silva MM. Effects of low-level laser therapy at wavelengths of 660 and 808 nm in experimental model of osteoarthritis. Photochem Photobiol 2012;88:161–166.
13. Hanlon EB, Manoharan R, Koo TW, et al. Prospects for in vivo Raman spectroscopy. Phys Med Biol 2000;45:R1–R59.
14. Tu Q, Chang C. Diagnostic applications of Raman spectroscopy. Nanomedicine 2012;8:545–558.
15. Peres MB, Silveira L Jr, Zângaro RA, Pacheco MT, Pasqualucci CA. Classification model based on Raman spectra of selected morphological and biochemical tissue constituents for identification of atherosclerosis in human coronary arteries. Lasers Med Sci 2011;26:645–655.
16. Souza RA, Xavier M, da Silva FF, et al. Influence of creatine supplementation on bone quality in the ovariectomized rat model: an FT-Raman spectroscopy study. Lasers Med Sci 2012;27:487–495.

17. Lim NS, Hamed Z, Yeow CH, Chan C, Huang Z. Early detection of biomolecular changes in disrupted porcine cartilage using polarized Raman spectroscopy. J Biomed Opt 2011;16:017003.
18. Ellis R, Green E, Winlove CP. Structural analysis of glycosaminoglycans and proteoglycans by means of Raman microspectrometry. Connect Tissue Res 2009;50:29–36.
19. Dehring KA, Smukler AR, Roessler BJ, Morris MD. Correlating changes in collagen secondary structure with aging and defective type II collagen by Raman spectroscopy. Appl Spectrosc 2006;60:366–372.
20. Bonifacio A, Sergo V. Effects of sample orientation in Raman microspectroscopy of collagen fibers and their impact on the interpretation of the amide III band. Vib Spectrosc 2010;2:314–317.
21. Esmonde–White KA, Esmonde–White FW, Morris MD, Roessler BJ. Fiber-optic Raman spectroscopy of joint tissues. Analyst 2011;136:1675–1685.
22. Esmonde–White KA, Mandair GS, Raaii F, et al. Raman spectroscopy of synovial fluid as a tool for diagnosing osteoarthritis. J Biomed Opt 2009;14:034013.
23. Souza RA, Xavier M, Mangueira NM, et al. Raman spectroscopy detection of molecular changes associated with two experimental models of osteoarthritis in rats. Lasers Med Sci 2014;29:797–804.
24. Kerns JG, Gikas PD, Buckley K, et al. Evidence from Raman spectroscopy of a putative link between inherent bone matrix chemistry and degenerative joint disease. Arthritis Rheumatol 2014;66:1237–1246.
25. Morris MD, Mandair GS. Raman assessment of bone quality. Clin Orthop Relat Res 2011;469:2160–2169.
26. McCreadie BR, Morris MD, Sudhaker CTC, et al. Bone tissue compositional differences in women with and without osteoporotic fracture. Bone 2006;39:1190–1195.
27. Kunstar A, Leijten J, van Leuveren S, et al. Recognizing different tissues in human fetal femur cartilage by label-free Raman microspectroscopy. J Biomed Opt 2012;17: 116012.
28. Silveira L Jr, Sathaiah S, Zângaro RA, Pacheco MC, Pasqualucci CA. Correlation between near-infrared Raman spectroscopy and the histopathological analysis of atherosclerosis in human coronary arteries. Lasers Surg Med 30; 2002:290–297.
29. Bodanese B, Silveira FL, Zângaro RA, Pacheco MT, Pasqualucci CA, Silveira L. Discrimination of basal cell carcinoma and melanoma from normal skin biopsies in vitro through Raman spectroscopy and principal component analysis. Photomed Laser Surg 2012;30:381–387.
30. Lee C, Wen C, Yc C, et al. Intra-articular magnesium sulfate (MgSO4) reduces experimental osteoarthritis and nociception: association with attenuation of Nmethyl-D-aspartate (NMDA) receptor subunit 1 phosphorylation and apoptosis in rat chondrocytes. Osteoarthr Cartil 2009;17:1485–1493.
31. Xavier M, de Souza RA, Pires VA, et al. Low-level light-emitting diode therapy increases mRNA expressions of IL-10 and type I and III collagens on Achilles tendinitis in rats. Lasers Med Sci 2014;29:85–90.
32. Tarnowski CP, Ignelzir MA Jr, Wang W, Taboas JM, Goldstein SA, Morris MD. Earliest mineral and matrix changes in force-induced musculoskeletal disease as revealed by Raman microspectroscopic imaging. J Bone Miner Res 2004;19:64–71.
33. Steiner R, Laser–tissue interactions. In: Laser and IPL Technology in Dermatology and Aesthetic Medicine. S Karsai, C Raulin C (eds.). Berlin, Heidelberg, Netherlands: Springer, 2011, pp. 23–36.
34. Palmer AJ, Brown CP, McNally EG, et al. Non-invasive imaging of cartilage in early osteoarthritis. Bone Joint J 2013;95-B:738–746.
35. Junqueira LC, Carneiro J. Cartilaginous tissue. In: Basic Histology–Text & Atlas, 11th ed. Rio de Janeiro: Guanabara Koogan, 2011, pp. 129–134.
36. Aparecida Da Silva A, Leal–Junior EC, Alves AC, et al. Wound-healing effects of low-level laser therapy in diabetic rats involve the modulation of MMP-2 and MMP-9 and the redistribution of collagen types I and III. J Cosmet Laser Ther 2013;15:210–216.
37. Movasaghi Z, Rehman S, Rehman IU. Raman spectroscopy of biological tissues. Appl Spectrosc Rev 2007;42:493–541.
38. Merashly M, Uthman I. Management of knee osteoarthritis: an evidence-based review of treatment options. J Med Liban 2012;60:237–242.
39. Takahashi Y, Sugano N, Takao M, Sakai T, Nishii T, Pezzotti G. Raman spectroscopy investigation of load-assisted microstructural alterations in human knee cartilage: Preliminary study into diagnostic potential for osteoarthritis. J Mech Behav Biomed Mater 2013;31:77–85.
40. Huber M, Trattnig S, Lintner F. Anatomy, biochemistry, and physiology of articular cartilage. Invest Radiol 2000;35: 573–580.
41. Moita Neto JM, Moita GC. Introduction to an exploratory analysis of multivariate date. Quim Nova 1998;21:467–469.
42. Sikirzhytski V, Virkler K, Lednev IK. Discriminant analysis of Raman spectra for body fluid identification for forensic purposes. Sensors 2010;10:2869–2884.
43. Sobol E, Shekhter A, Guller A, Baum O, Baskov A. Laser-induced regeneration of cartilage. J Biomed Opt 2011;16: 080902.
44. Mankin HJ. The response of articular cartilage to mechanical injury. J Bone Joint Surg Am 1982;64:460–466.
45. Alves ACA, Albertini R, dos Santos SA, et al. Effect of low-level laser therapy on metalloproteinase MMP-2 and MMP-9 production and percentage of collagen types I and III in a papain cartilage injury model. Lasers Surg Med 2014;29:911–919.
46. Sun Y, Mauerhan DR, Kneisl JS, et al. Histological examination of collagen and proteoglycan changes in osteoarthritic menisci. Open Rheumatol J 2012;6:24–32.
47. Adam M, Deyl Z. Altered expression of collagen phenotype in osteoarthrosis. Clin Chim Acta 1983;133:25–32.
48. Pallotta RC, Bjordal JM, Frigo L, et al. Infrared (810-nm) low-level laser therapy on rat experimental knee inflammation. Lasers Med Sci 2012;27:71–78.
49. Samoilova KA, Zhevago NA, Petrishchev NN, Zimin AA. Role of nitric oxide in the visible light-induced rapid increase of human skin microcirculation at the local and systemic levels: II. healthy volunteers. Photomed Laser Surg 2008;26:4439.

Address correspondence to:
Antonio Balbin Villaverde
Instituto de Engenharia Biomédica
Universidade Camilo Castelo Branco - UNICASTELO.
Estr. Dr. Altino Bondesan, 500
12247-016, São José dos Campos, SP
Brazil

E-mail: abvillaverde@gmail.com